Donors in multivalley semiconductors in the zero-radius center-cell approximation

I. L. Beĭnikhes and Sh. M. Kogan

Institute of Radio Engineering and Electronics, USSR Academy of Sciences
(Submitted 16 November 1986)
Zh. Eksp. Teor. Fiz. **93**, 285–301 (July 1987)

We obtain the wave functions of the ground states of group-V shallow donors in Ge and Si in the zero-radius center cell (ZRCC) approximation, with allowance for the anisotropy of the electron effective mass. The distances between the energy levels of odd excited states, calculated in the effective-mass approximation, agree with the distances between the corresponding spectral lines to within the same accuracy with which the locations of these lines have been measured. Two odd states ($6P_{\pm}$ and $9P_{\pm}$) previously unobserved in the spectra were found in the doors for Ge, and served to refine the identification of the spectral lines. The line intensities depend strongly on the depth E_i of the ground level of the impurity. Orthonormalized wave functions of the continuous spectrum were calculated and used to determine the spectra of the cross sections for photoionization of donors with different E_i. The polarizability of the donors were also obtained in the ZRCC approximation, as well as the changes of the valley-orbit splittings 4Δ of the ground levels with change of the magnetic field. The accuracy ($\lesssim 10\%$) of the ZRCC approximation was estimated for the ground levels of the donors in Ge and Si was estimated by comparison with the experiments.

1. INTRODUCTION

Shallow impurity centers in semiconductors are known to be described in the effective-mass approximation (EMA).[1,2] It is also known, however, that the ground-state energy of a shallow impurity center differs from the lowest eigenvalue of the corresponding EMA equation, and this difference is not the same for different impurities of the same type in one and the same semiconductor.[2] This effect was named the chemical shift. Obviously, its cause is that the condition for the validity of the EMA (smoothness of the perturbation introduced by the impurity into the crystal) is violated in the region of the crystal central cell that contains the impurity atom. The chemical shift is therefore also referred to as the center-cell correction (CCC). The theoretical calculation of the CCC for the ionization energies of shallow impurities in semiconductors is the subject of many studies (see, e.g., the review paper[3]), but the problem still remains unsolved.

Many characteristics of shallow impurities (in contrast to the ground-state energy) are determined almost entirely by the behavior of the wave function outside the center cell—in a region where the potential of the impurity is smooth and the wave function satisfies the EMA equations. These quantities include the oscillator strengths (intensities) of optical transitions, the photoionization cross section, the polarizability, and the diamagnetic level shifts in a magnetic field. The first three quantities are expressed in terms of the matrix elements of the dipole moment between the ground state (even) and odd excited states, whose wave functions are close to zero in the region of the central cell. In addition, the product of the radial functions of the ground and excited states is multiplied in these matrix elements by r^3 (r is the distance from the central cell). The diamagnetic shift is expressed in terms of integrals with respect to r, which contain r^4. This suggests that the center-cell region (small r of the order of or less than the dimension a_0 of the unit cell of the crystal) makes a small contribution to the quantities listed above.

This raises the question of calculating the wave function of the ground state in the EMA outside the central cell, with allowance for the true level energy, which can at present be obtained only from experiment. Since the ground-level energy is not equal to an eigenvalue of the EPM equation, in view of the CCC, the sought wave function should diverge as $r \to 0$ (the bound as $r \to \infty$ remains unchanged). If the shallow impurity is hydrogenlike (the corresponding band edge is not degenerate and the effective mass is isotropic), at a given ground-level energy, the EMA equation has a single solution that is bounded as $r \to \infty$ and diverges as $r \to 0$ (for a nonzero CCC), and this solution diverges like r^{-1}, i.e., is normalized.[4] In the case of hydrogenlike shallow impurity centers (donors in multivalley semiconductors, acceptors in semiconductors with degenerate valence-band edge, i.e., in all cubic semiconductors), a host of bounds exist on the solutions of the EMA (at nonzero CCC). Indeed, in this case the expansion of the wave function of the donor ground state in the spherical harmonics Y_{LM} (in the $L-S$ coupling functions in the case of acceptors) contain not only terms with $L=0$, but also terms with even $L>0$, so that the EMA equations have solutions that diverge as $r \to 0$ approximately like r^{-L-1}. Strictly speaking, a unique solution could be obtained by matching the solution outside the central cell ($r \gg a_0$), where the EMA is valid, to the solution in the central-cell region ($r \lesssim a_0$). The latter, however, is not known at all.

We use the fact that usually the dimension a_0 of the central cell is small compared with the effective Bohr radius a even in the case when the CCC to the ground-state energy is appreciable. In the limit $a_0/a \to 0$ the normalized solution should increase as $r \to 0$ not faster than r^{-1}. This condition singles out the only solution of the EMA equation. For the reason indicated above, it can be called the zero-radius central cell (ZRCC) approximation. It is similar to the quantum-defect method.

The ZRCC approximation was used earlier for calculation of shallow acceptors in the spherical approximation.[5] In this case the problem reduces to solution of a system of only

 0038-5646/87/070164-10$04.00

two ordinary differential equations (ODE) of second order, which made it possible to find all the fundamental solutions near $r=0$ and readily eliminate the one that diverges like r^{-3}. We show in the present paper, with shallow donors in multivalley semiconductors as the example, how to find the solution needed in the ZRCC approximation in the general case, when the EMA equation is a partial differential equation with nonseparable variables, or a system of such equations. Besides the donors in semiconductors with anisotropic effective mass, such systems include also acceptors in those cases when account must be taken of the nonsphericity of the hole bands, and also all the shallow impurities in a magnetic field. In addition, shallow donors in multivalley semiconductors are rather important objects in semiconductor physics, and their detailed quantum calculation in the present paper is of interest in itself.

We shall see that many characteristics of shallow donors depend strongly on the ionization energy of these impurities. It is therefore important that it is possible to determine, within the scope of the ZRCC approximation, the characteristic of each specific shallow impurity, if its ionization energy is known (from experiment). It is important, that in these calculations there is no possibility whatever of adjusting the parameters of the center-cell potential. The accuracy of the ZRCC approximation must be estimated by comparing the calculated values with those experimental data whose accuracy is high enough. This permits an assessment of the accuracy of the results of this approximation and of those obtained when there are no sufficiently accurate measurements and the calculation results are absolutely necessary. We shall calculate the polarizabilities of various donors in Ge and Si (Sec. 5) and the dependence of the valley-orbit splitting of the donor levels on the magnetic field (Sec. 6), and verify by comparing the results with experiment that the accuracy of the ZRCC approximation is high enough. This permits an assessment of the accuracy of the oscillator strengths calculated in Sec. 3 for the optical transitions in the same impurities (to our knowledge there are no quantitative experimental data) and of the cross sections calculated in Sec. 4 for the donor photoionization (the accuracy of their measured absolute values is as yet low).

2. SYSTEM OF EQUATIONS

The EMA Hamiltonian for donors in a multivalley semiconductor is

$$\hat{H}=-\frac{\hbar^2}{2}\left[\frac{1}{m_t}\left(\frac{\partial^2}{\partial x^2}+\frac{\partial^2}{\partial y^2}\right)+\frac{1}{m_l}\frac{\partial^2}{\partial z^2}\right]-\frac{e^2}{\varkappa r}. \tag{1}$$

Here m_1 and m_2 are the transverse and longitudinal effective masses, and $\varkappa$ is the dielectric constant of the semiconductor. The variables in the Schrödinger equation with Hamiltonian (1) do not separate and no analytic solution is possible.

We transform to a deformed coordinate frame and to dimensionless variables (as in Ref. 6)

$$\begin{gathered}\tilde{x}=\gamma^{1/6}x/a,\quad \tilde{y}=\gamma^{1/6}y/a,\quad \tilde{z}=\gamma^{-1/3}z/a,\\ a=\gamma^{1/6}\hbar^2\varkappa/m_t e^2,\quad \gamma\equiv m_l/m_t,\\ \tilde{r}=(\tilde{x}^2+\tilde{y}^2+\tilde{z}^2)^{1/2},\quad \cos\theta=\tilde{z}/\tilde{r}.\end{gathered} \tag{2}$$

In this notation the EMA equation takes the form

$$(\tilde{\Delta}/2+q(\theta)/\tilde{r}+\tilde{E})\psi(\tilde{\mathbf{r}})=0, \tag{3}$$

where E is the dimensionless energy in units of $E_d=m_t e^4/\hbar^2\varkappa^2$, and

$$q(\theta)=[1-(1-\gamma)\cos^2\theta]^{-1/2}. \tag{4}$$

Equation (3) differs from the equation with Hamiltonian (1) in that the anisotropy of the problem is transferred in it from the kinetic-energy operator to that of the potential energy. This will be shown below to simplify the calculation.

We represent the sought wave function as an expansion in spherical harmonics with definite parity P and projection M of the angular momentum:

$$\psi^{(PM)}(\tilde{r},\theta,\varphi)=\sum_{L\geqslant L_{min}} R_L^{(PM)}(\tilde{r})\,Y_{LM}(\theta,\varphi). \tag{5}$$

The summation in (5) is over quantum numbers L of a definite parity that coincides with the parity P of the state, $L_{\min}\geqslant|M|$ is the minimum value of L, and $R_L^{(PM)}(\tilde{r})$ are radial functions that satisfy, as follows from (3), the ODE system:

$$\left[\frac{d^2}{d\tilde{r}^2}+\frac{2}{\tilde{r}}\frac{d}{d\tilde{r}}-\frac{L(L+1)}{\tilde{r}^2}+2\tilde{E}\right]R_L^{(PM)}$$
$$+\frac{2}{\tilde{r}}\sum_{L'\geqslant L_{min}} q_{LL'}^{(PM)}R_{L'}^{(PM)}=0. \tag{6}$$

Here $q_{LL'}^{(PM)}=\langle LM|q(\theta)|L'M\rangle$. In the choice of the Y_{LM} phases we follow Ref. 7.

In the expansion (5), the terms with large L describe fast angular oscillations of the wave functions. Since a high positive energy is associated with these oscillations, these terms should be small and must not be in highly excited states. This allows us to discard in (5) all the terms containing L exceeding a certain sufficiently large $L_{\max}$ that depends on the considered energy level. The system (6) becomes finite, and the number of second-order ODE in it will be designated N.

The same problem can be solved also without changing to the deformed system of coordinates (2). To this end, the Hamiltonian must be represented in the form

$$\hat{H}=\hat{H}^{(0)}+\hat{H}^{(2)},$$
$$H^{(0)}=\frac{p^2}{2\bar{m}}-\frac{e^2}{\varkappa r},\quad \hat{H}^{(2)}=-\frac{3(1-\gamma)}{2+\gamma}\frac{1}{2\bar{m}}\left(p_z^2-\frac{1}{3}p^2\right), \tag{7}$$

$$\bar{m}^{-1}=(2m_t^{-1}+m_l^{-1})/3. \tag{8}$$

In a spherical-harmonics basis the matrix $H^{(0)}$ is diagonal, the matrix $H^{(2)}$ is tridiagonal, and calculation of their matrix elements is elementary. The results are, naturally, the same as when the system (2)–(6) is used, but a large basis is required in the latter to obtain the same accuracy.

We solve the system (6) by a non-variational method of transferring the condition of finite solutions from the singular point (see the review paper[8] and also Ref. 9; the idea of the method as applied to our problem is described in Ref. 10 and in the Appendix).

3. ENERGY AND INTENSITY OF THE LINES IN THE OPTICAL ABSORPTION SPECTRA

If the impurity center is shallow, the rates of the optical transitions between its states under the influence of an electromagnetic wave with photon energies $h\nu \ll E_g$ (E_g is band gap) are determined by the smooth (macroscopic) part of the electric field of the wave. The cross section for the dipole optical absorption connected with transitions from the ground state of energy E_0 to excited states with energies E_n is equal to (**e** is the polarization unit vector)[11]

$$\sigma(h\nu) = \frac{4\pi^2 e^2 \omega}{c\varkappa^{1/2}} \sum_n |(\mathbf{er})_{0n}|^2 \delta(E_n - E_0 - h\nu). \quad (9)$$

We consider first the cross section for optical transitions in one valley of the conduction band. This cross section $\sigma_v(\mathbf{e},h\nu)$ (v is the number of the valley) depends on the orientation of **e** relative to the valley axis. If practically the entire absorption by the shallow impurity centers is exhausted by the photon energies $h\nu \ll E_g$, the area under the entire spectrum of the cross section $\sigma_v(\mathbf{e},h\nu)$ is equal to[11]

$$\int_0^{E_g} dh\nu \sigma_v(\mathbf{e}, h\nu) = \frac{2\pi^2\hbar e^2}{c\varkappa^{1/2}} e_i m_{ik}^{-1} e_k, \quad (10)$$

i.e., it is determined by the reciprocal effective mass in the radiation-polarization direction (m_{ik}^{-1} is the reciprocal-effective-mass tensor). The sum rule (10) is determined by the mass m_l and by the mass m_t respectively, for the cross sections σ_l and σ_t in the case of longitudinal and transverse polarizations.

The ground state of an undeformed multivalley semiconductor is known to be a symmetric superposition of functions of all n_v valleys. By virtue of the cubic symmetry, the observed absorption cross section is equal to

$$\sigma(h\nu) = (2\sigma_t + \sigma_l)/3. \quad (11)$$

It follows from (10) that it satisfies the sum rule

$$\int_0^{E_g} dh\nu \sigma(h\nu) = 2\pi^2\hbar e^2/c\varkappa^{1/2}\bar{m} = 1{,}0976 \cdot 10^{-13} [\text{meV}\cdot\text{cm}^2] \varkappa^{-1/2}(m_0/\bar{m}), \quad (12)$$

where $\bar{m}^{-1}$ is the average reciprocal effective mass (8).

The sum rules (10) and (12) are valid also if the center cell is represented in the effective-mass equation by some short-range potential. In particular, they are valid also in the ZRCC approximation.

The fraction of the entire area (12) allotted to the a given line (the oscillator strength) can be expressed in terms of integral of the radial functions $R_L(\tilde{r})$ of the initial ground state ($L = 0, 2, \ldots$) and of the radial functions $F_L^{(M)}(\tilde{r})$ the final state ($L = 1, 3, \ldots$):

$$f(nP_0) = \frac{2\gamma}{2+\gamma} [\bar{E}(nP_0) - \bar{E}_0] \left| \sum_{L\geq 1} \int_0^\infty d\tilde{r} \tilde{r}^3 F_L^{(0)}(\tilde{r}) \bar{R}_L^{(0)}(\tilde{r}) \right|^2,$$

$$f(nP_\pm) = \frac{4}{2+\gamma} [\bar{E}(nP_\pm) - \bar{E}_0] \left| \sum_{L\geq 1} \int_0^\infty d\tilde{r} \tilde{r}^3 F_L^{(1)}(\tilde{r}) \bar{R}_L^{(1)}(\tilde{r}) \right|^2. \quad (13)$$

Odd states with $M = 0$ are designated here by nP_0 ($n = 2, 3, \ldots$) and those with $M = \pm 1$ by $nP_\pm$. It is assumed that the radial functions have been calculated in the system (2). For brevity, we have introduced in (13) the notation

$$\bar{R}_L^{(0)} = \frac{1}{(2L+1)^{1/2}} \left\{ \frac{L}{(2L-1)^{1/2}} R_{L-1} + \frac{L+1}{(2L+3)^{1/2}} R_{L+1} \right\},$$

$$\bar{R}_L^{(1)} = \left[\frac{L(L+1)}{2(2L+1)} \right]^{1/2} \left\{ \frac{1}{(2L-1)^{1/2}} R_{L-1} - \frac{1}{(2L+3)^{1/2}} R_{L+1} \right\}. \quad (14)$$

Tables I and II list the level energies $E(nP_M)$ and the oscillator strengths (OS) $f(nP_M)$ obtained by us for shallow donors in Ge and Si. For more reliable identification of the experimentally observed lines, the solid lines in Fig. 1 show the dependences of the energies $E(nP_\pm)$ on $\gamma = m_t/m_l$ while the dashed lines show the dependences obtained by Faulkner[12] by a variational method (the interpretations of all experiments since 1969 were based on the results of Ref. 12). The solid horizontal strokes on the left show the measured values of the levels in Ge, and the dashed ones show the levels obtained by us but not noted in the experiments.

With decrease of γ, the energy levels calculated in Ref. 12 deviate increasingly from our calculated values (Fig. 1). In the case of Si, the inaccuracy in Ref. 12, while higher than experimental, was nevertheless smaller than the distances between the neighboring levels and therefore did not lead to incorrect line identification. At $\gamma = \gamma_{Ge}$ the deviation of the energies $E(nP_\pm)$ calculated in Ref. 12 from those calculated by us and from experiment at $n > 5$ become of the same order of and larger than the distances between neighboring levels. This led in fact to an incorrect identification of all the transitions, starting with $6P_\pm$. The erroneous interpretation of the donor spectra in Ge on the basis of Ref. 12 remained unnoticed,[1)] in particular, because the transitions to $6P_\pm$ and $9P_\pm$ were left out of the experiments, and some of the levels calculated in Ref. 12 for Ge ($5f_\pm$ and $6f_\pm$ in the notation of Ref. 12) turned out accidentally next to the experimental points (Fig. 1) corresponding actually to other states ($6p_\pm$ and $7p_\pm$ in the same notation). On the other hand, the lines $6P_\pm$ and $9P_\pm$ were left out because the corresponding OS were several times smaller than the OS of the neighboring lines $5P_\pm$ and $8P_\pm$ (Table I). The OS, however, are not so small as to make these lines practically unobservable, as for example in the case of $12P_\pm$ in Ge and $9P_\pm$ in Si (Tables I and II).

Following Ref. 12, we obtained the dielectric constant $\varkappa$ of germanium from the condition of best agreement between the calculated levels and experiment.[14,15] We obtained $\varkappa = 15.40$, somewhat higher than the 15.36 obtained in Ref. 12 from the experimental $2P_\pm - 2P_0$ energy difference. At $\varkappa = 15.40$, i.e., $E_d = 9.352$ meV, the $nP_\pm$ levels of the donors in Ge, obtained by us, agree with all those measured in Refs. 14 and 15 within the limits of experimental error $\lesssim 5$ μeV (for a comparison with experiments see Ref. 16).

It can therefore be concluded from a comparison of the results of Table I with experiment that the odd donor states in Ge are described in the EMA with accuracy not worse than that of spectroscopic experiments.[14,15]

In Table III are gathered, for comparison of the theory with experiments on Si, data obtained by various workers for the differences $E(nP_M) - E(2P_\pm)$. It can be seen that the

TABLE I. Energy levels E of odd states of shallow donors in Ge and oscillator strengths of optical transitions from the ground level $1s\,(A_1)$. The parentheses contain the level designations used in Ref. 12; the number under the impurity symbol is the ionization energy in meV ($E_d = 9.352$ meV).

Levels	$\lvert E\rvert/E_d$	$\lvert E\rvert$, meV	$f\,(nP_M)\cdot 10^3$			
			EMA 9.783	Sb 10.46	P 12.88	As 14.16
$2P_0(2p_0)$	0.5079	4.750	18.8	17.2	12.4	10.5
$3P_0(3p_0)$	0.2752	2.573	1.91	2.07	2.16	2.05
$2P_\pm(2p_\pm)$	0.1839	1.720	233	202	126	102
$4P_0(4p_0)$	0.1806	1.689	0.648	0.738	0.852	0.838
$5P_0(4f_0)$	0.1301	1.217	0.316	0.368	0.446	0.446
$3P_\pm(3p_\pm)$	0.1109	1.037	40.6	36.4	25.0	20.7
$6P_0(5p_0)$	0.0992	0.928	0.184	0.217	0.270	0.272
$7P_0(5f_0)$	0.0856	0.800	$1.7\cdot10^{-3}$	$1.6\cdot10^{-3}$	$1.3\cdot10^{-3}$	$1.2\cdot10^{-3}$
$4P_\pm(4p_\pm)$	0.0802	0.750	21.8	19.8	14.0	11.7
$8P_0(6p_0)$	0.0786	0.735	0.116	0.138	0.176	0.180
$5P_\pm(4f_\pm)$	0.0649	0.607	20.3	18.2	12.6	10.5
$6P_\pm(5p_\pm)$	0.0613	0.573	2.26	2.13	1.63	1.40
$7P_\pm(5f_\pm)$	0.0499	0.467	7.11	6.56	4.80	4.07
$8P_\pm(6p_\pm)$	0.0426	0.399	7.44	6.72	4.78	4.02
$9P_\pm(6f_\pm)$	0.0410	0.384	1.40	1.32	1.01	0.88
$10P_\pm(6h_\pm)$	0.0350	0.328	5.71	5.27	3.86	3.28
$11P_\pm(7p_\pm)$	0.0335	0.313	2.01	1.86	1.27	1.05
$12P_\pm(7f_\pm)$	0.0310	0.290	0.16	0.14	0.10	0.083
$13P_\pm(7h_\pm)$	0.0302	0.282	2.28	2.12	1.60	1.37
$14P_\pm(8p_\pm)$	0.0267	0.250	2.80	2.56	1.85	1.57
$15P_\pm(8f_\pm)$	0.0261	0.244	0.79	0.75	0.58	0.50
$16P_\pm(8h_\pm)$	0.0233	0.217	2.87	2.62	1.87	1.57
$17P_\pm(8k_\pm)$	0.0221	0.207	1.44	1.36	1.04	0.90

lowest odd $2P_0$ levels of different donors differ possibly by as much as $\sim 100\,\mu$eV. The differences of the higher levels for different donors are of the same order as the difference between data of different workers for one and the same donor ($\sim 10 - 20\,\mu$eV). As seen from Table III, the odd states of donors in Si above $2P_0$ are described by the EMA with the same accuracy, which amounts to less than 10^{-3} of the donor ionization energy in Si.

We proceed now to analyze the line intensities. Transitions to the nP_0 level are produced in each conduction-band valley by the radiation electric-vector component parallel to the valley axis, in the direction of which the effective mass is a maximum. Therefore the oscillator strengths (OS) of such lines are lower than the OS of lines corresponding to transitions to $nP_\pm$ levels having approximately the same or even higher energy. This effect is particularly large in Ge, viz., the OS of the transitions to levels nP_0 with $n \geqslant 4$ are negligible. For example, $f(4P_0)$ is one-third as large than the OS of the last of the identified lines ($11P_\pm$). This explains why only two nP_0 lines ($n = 2$ and 3) as can be seen in the donor spectra of Ge. While the effect in Si is less pronounced because of the lower effective-mass anisotropy, it is nontheless significant: $f(nP_0) < 10^{-3}$ starting with $n = 7$ (but also at $n = 5$).

The oscillator strengths $f(nP_\pm)$ vary nonmonotonically with increase of the number n (Tables I and II), in accord with the experiments. It should be noted that Ge do-

TABLE II. Energy levels E of odd states of shallow donors in Si and oscillator strengths of optical transitions from the ground level $1s\,(A_1)$. The parentheses contain the level designations used in Ref. 12; the number under the impurity symbol is the ionization energy in meV ($E_d = 39.88$ meV).

Levels	$\lvert E\rvert/E_d$	$\lvert E\rvert$, meV	$f\,(nP_M)\cdot 10^3$			
			EMA 31.270	Sb 42.74	P 45.59	As 53.76
$2P_0(2p_0)$	0.28810	11.491	57.9	35.1	31.3	23.0
$2P_\pm(2p_\pm)$	0.16050	6.401	287	153	133	93.4
$3P_0(3p_0)$	0.13753	5.485	7.81	6.86	6.44	5.2[illegible]
$4P_0(4p_0)$	0.08297	3.309	2.75	2.68	2.55	2.16
$3P_\pm(3p_\pm)$	0.07822	3.120	53.9	33.9	30.4	22.5
$5P_0(4f_0)$	0.05864	2.339	0.057	0.052	0.049	0.042
$6P_0(5p_0)$	0.05603	2.235	1.27	1.30	1.25	1.08
$4P_\pm(4p_\pm)$	0.05483	2.187	18.7	12.1	10.8	8.09
$5P_\pm(4f_\pm)$	0.04749	1.894	6.00	4.09	3.70	2.80
$7P_0(5f_0)$	0.04089	1.631	0.74	0.77	0.74	0.65
$8P_0(6p_0)$	0.03785	1.510	0.014	0.017	0.017	0.015
$6P_\pm(5p_\pm)$	0.03634	1.449	14.9	10.1	9.09	6.87
$7P_\pm(5f_\pm)$	0.03158	1.259	0.594	0.37	0.33	0.24
$9P_0(6f_0)$	0.03116	1.243	0.48	0.51	0.49	0.43
$8P_\pm(6p_\pm)$	0.02684	1.071	6.89	4.74	4.30	3.27
$9P_\pm(6f_\pm)$	0.02513	1.002	$4\cdot10^{-4}$	$<10^{-4}$	$<10^{-4}$	$<10^{-4}$
$10P_\pm(6h_\pm)$	0.02222	0.886	3.64	2.43	2.20	1.66
$11P_\pm(7p_\pm)$	0.02064	0.823	2.26	1.44	1.30	0.97
$12P_\pm(7f_\pm)$	0.01880	0.750	1.41	0.90	0.81	0.61
$13P_\pm(7h_\pm)$	0.01699	0.678	2.69	1.74	1.57	1.19
$14P_\pm(8p_\pm)$	0.01597	0.637	$7\cdot10^{-4}$	0.003	0.003	0.003
$15P_\pm(8f_\pm)$	0.01494	0.596	2.39	1.50	1.35	1.00
$16P_\pm(8h_\pm)$	0.01419	0.566	0.95	0.63	0.57	0.43

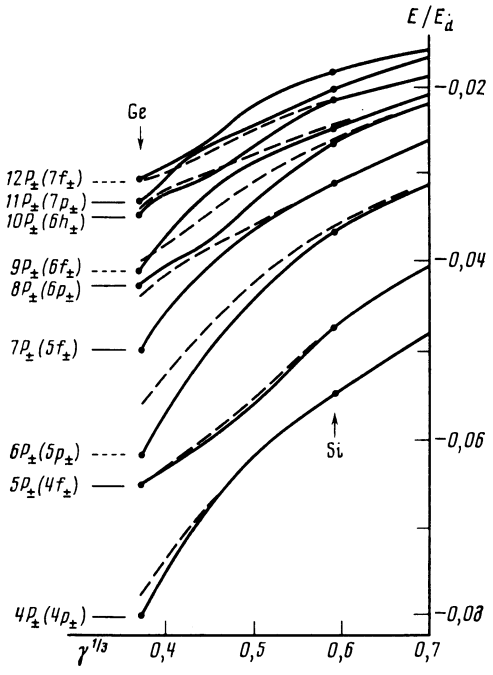

FIG. 1. Dependence of the energy of odd states $nP_{\pm}$ on the effective-masses anisotropy parameter γ. Solid curves—present calculation, dashed—result of Ref. 12. The arrows correspond to the values of γ for Si and Ge. The solid and dashed horizontal lines mark respectively the experimental[14,15] values of the level energy and the levels to which transitions were not observed.

nors have, above the last level identified in experiment ($11P_{\pm}$), levels transitions to which have OS that are also large to permit their identification ($n = 13, 14, 16$).

The OS of the brightest lines ($2P_0$ and $nP_{\pm}$) decrease greatly with increased depth E_i of the ground level of the impurity, since its wave function is in this case more and more concentrated in a region near the center cell, where the wave function of the final state for a dipole optical transition (odd) is close to zero, and the matrix element of the dipole moment decreases. This effect is very strong (see Tables I and II) and must be taken into account in applied spectroscopy of shallow impurities. It is of interest, however, that the dependence of $f(3P_0)$ on E_i is relatively weak (and is even nonmonotonic in Ge).

Since the intensities of different lines depend differently on E_i, their ratios are also subject to a significant "chemical effect." For example, in Si the ratio $f(3P_0)/f(3P_{\pm})$ is ≈ 0.14 for Li impurity atoms and ≈ 0.24 for As impurities. The analogous ratio is ≈ 0.057 for Sb inGe and ≈ 0.10 for As in Ge.

4. SPECTRA OF PHOTOEFFECT FROM DONOR ATOMS

The spectra of the cross sections for photoionization of non-hydrogenlike impurities are of considerable interest both for spectroscopy of shallow impurities and for physics of IR receivers based on doped semiconductors. The photoionization spectra of donors in multivalley semiconductors was never calculated before, since there was no general method whatever of calculating orthonormalized wave functions of the continuous spectrum of non-hydrogenlike quantum systems. Such a method, using the condition of finite solutions at infinity, was developed by us earlier.[10,20]

The known degeneracy of the continuum states is manifest by the fact that at each energy $E > 0$, parity P the components of the angular momentum M along the valley axis Z, and number v of the valley there exist N different mutually orthogonal solutions of the Schrödinger (N is the number of terms retained in the expansion of the wave function in spherical harmonics, see Sec. 2). Let $l = 1, \ldots N$ be the number of each such solution, and let the continuum functions $\psi^{(EPMvl)}$ be normalized to $\delta(E - E')$. It follows then from (9) that the cross sections σ_t and σ_l of the intravalley dipole optical transitions are equal to

$$\sigma_t(h\nu) = \sigma_d(\bar{E}+\bar{E}_i) \sum_l \left| \sum_{L\geqslant 1} \int_0^\infty d\tilde{r}\tilde{r}^3 F_L^{(E1l)}(\tilde{r})\, \bar{R}_L^{(1)}(\tilde{r}) \right|^2,$$

$$\sigma_l(h\nu) = \sigma_d\gamma(\bar{E}+\bar{E}_i) \sum_l \left| \sum_{L\geqslant 1} \int_0^\infty d\tilde{r}\tilde{r}^3 F_L^{(E0l)}(\tilde{r})\, \bar{R}_L^{(0)}(\tilde{r}) \right|^2. \tag{15}$$

The cross section is here

$$\sigma_d = 4\pi^2\hbar^3\varkappa^{1/2}/cm_t^2e^2, \tag{16}$$

$F^{(EMl)}(\tilde{r})$ ($L = 1,3, \ldots$) are the radial functions of the continuum, $R_L^{(M)}$ are combinations of radial functions of the ground state [see Eq. (14)], $E = h - E_i$, and E and E_i are dimensionless energies in units of E_d.

TABLE III. Measured energy levels $E(nP_M)$ of donors in silicon relative to the level $2P_{\pm}$ (in meV).

nP_M	P [17]	P [18]	Sb [17]	Sb [18]	Sb [19]	As [17]	As [18]	Li [18]	Li—O [18]
$2P_0$	−5.07	−5.08	−5.13	−5.13	–	−5.11	−5.10	−5.11	−5.17
$3P_0$	0.93	0.93	0.90	–	0.88	0.92	0.91	0.91	0.89
$4P_0$	3.09	3.09	3.07	–	3.05	3.10	3.09	3.08	3.07
$3P_{\pm}$	3.29	3.28	3.28	3.26	–	3.27	3.28	3.28	3.28
$5P_0$	4.08	4.07	–	–	–	–	–	–	–
$6P_0$	4.17	–	–	–	–	–	–	–	–
$4P_{\pm}$	4.22	4.21	4.20	–	4.18	4.20	4.21	4.20	4.20
$5P_{\pm}$	4.51	4.50	4.46	–	4.44	4.49	4.50	4.50	4.50
$7P_0$	4.76	4.75	4.70	–	4.67	–	–	4.76	4.74
$6P_{\pm}$	4.95	4.94	4.92	–	4.90	4.93	4.94	4.93	4.93
$7P_{\pm}$	5.15	5.14	–	–	–	5.13	–	5.15	5.11
$8P_{\pm}$	5.32	5.31	5.31	–	5.28	5.32	–	5.32	5.30
$10P_{\pm}$	5.52	–	–	–	–	–	–	–	–

It follows also from (9) that in an undeformed crystal the cross section of such a photoionization process, in which the electron lands in a definite valley v, is equal to (n_v is the total number of valleys)

$$\sigma^{(v)}(h\nu) = \frac{1}{n_v}\left[\frac{1}{3}(2\sigma_t+\sigma_l) - (\sigma_t-\sigma_l)\left(e_z^{(v)2} - \frac{1}{3}\right)\right]. \quad (17)$$

The total cross section of the photoeffect in the absence of deformation is given by (11).

The spectra, calculated from (11) and (15), of the cross sections for photoionization of shallow donors in Ge and Si, are shown in Fig. 2. With increasing ionization energy E_i, the cross section $\sigma(E_i)$ on the red boundary decreases (this effect was considered for the hydrogenlike model in Refs. 21 and 22) and at the same time the decrease of $\sigma(h\nu)$ with increase of $h\nu$ becomes less steep. We put $n = (E_i^{\text{EMA}}/E_i)^{1/2}$, where E_i^{EMA} is the ionization energy in the EMA. As seen from Fig. 3, in Ge at $n > \sim 0.7$ (and in Si at $n > \sim 0.6$) the maximum of $\sigma(h\nu)$ is on the red boundary $h\nu = E_i$ and the cross section decreases monotonically with increase of $h\nu$ (this takes place, in particular, for all donors of group V). At lower values of n the cross section passes through a maximum at $h\nu > E$, and the position of the maximum shifts towards larger $h\nu$ with decrease of n.

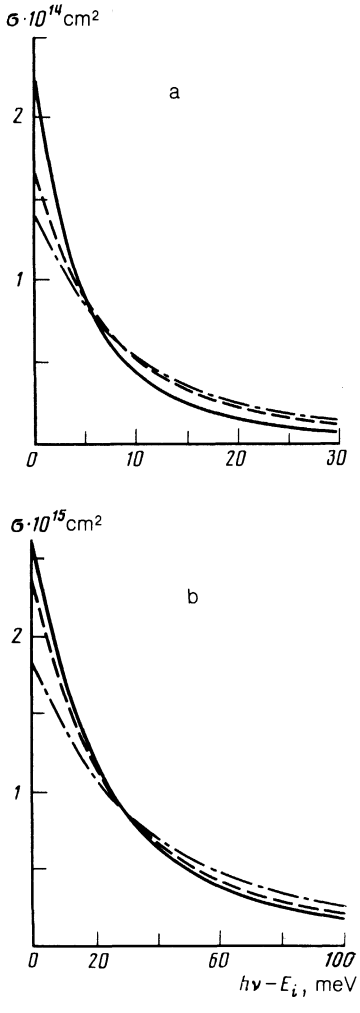

FIG. 2. Cross section for photoionization of shallow Sb (solid curve), P (dashed, and As (dash-dot) donors in Ge (a) and Si (b) vs the photon energy.

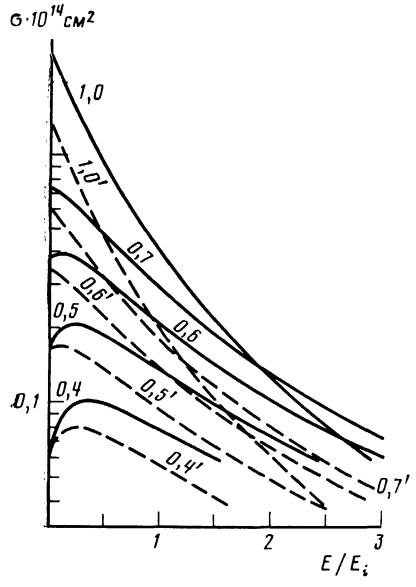

FIG. 3. Cross section for photoionization of donors to Ge vs the photon energy at different chemical shifts of the ground states. The curves are labeled by the values of the parameter $n = (E_i^{\text{EMA}}/E_i)^{1/2}$. Solid curves—calculation with allowance for anisotropy, dashed—calculation in isotropic model.

For the donors in Si, the theoretical and experimental[23] values (given in Ref. 24) of the cross sections for the photoeffect at the maximum are respectively (in units of 10^{-15} cm^2): 2.55 and 8.5 (Sb), 2.34 and 2.5 (P), and 1.81 and 1.6 (As). For the same impurities in Ge, the theoretical values of $\sigma(E_i)$ and those measured in Ref. 25 (and cited in Ref. 26) are equal to (in units of 10^{14} cm^2) 2.20 and 1.8 (Sb), 1.64 and 1.5 (P), and 1.40 and 1.1 (As). It can be seen that, except for Sb and Si, the deviation from experiment is not worse than $\sim 20\%$. The experimental values are hardly more accurate.

Since there was no method previously for calculating the cross sections of the photoeffect with allowance for the effective-mass anisotropy, it was calculated on the basis of the isotropic (hydrogenlike) model, using the electron mass determined from the known E_i^{EMA} (Refs. 21 and 23). It is of interest to compare the results of this model with a calculation that takes the mass anisotropy into account. Figure 3 shows the corresponding photoionization spectra of donors in Ge at different n. At $n = 1$ the exact cross section is double the cross section in the isotropic model (approximately 1.5 times larger in Si). With decrease of n, the exact cross section decreases more rapidly than the model value, so that the two cross section come closer together. The spectrum of the cross section, with anisotropy taken into account becomes nonmonotonic at larger values of n than in the spherical model.

It is of interest to track the variation of the fraction of the line spectrum, and accordingly the fraction of the continuum, in the total area (12) under the entire absorption spectrum with increase of the anisotropy and of the ground-level depth. In hydrogenlike atoms ($\gamma = 1$) it is known that the fractions of the line and continuous spectra are 0.565 and 0.545 of the entire sum (unity) of the oscillator strengths. The sums, listed in Table II, of the OS of the lines in the spectra of the donors in Si for the EMA, and for the Sb, P,

and As impurities, are respectively 0.47, 0.27, 0.24, and 0.18. The contribution of the transitions to even more excited states, estimated from the cross section for the photoeffect at $h\nu = E_i$, is ~0.01–0.02. The area under the calculated part of the continuum of the donors in Si ($h\nu < 31E_d$) yields according to (12) the respective values 0.52 (EMA), 0.71 (Sb), 0.74 (P), and 0.79 (As). It can be seen, first, that accurate to 1–3% the OS is equal to 1, thus providing an additional verification of the calculation accuracy. Second, with increase of E_i the fraction of the continuous spectrum in absorption increases, and the fraction of the line spectrum decreases.

For donors in Ge, the sums of the OS listed in Table I are 0.37 (EMA), 0.33 (Sb), 0.22 (P), and 0.18 (As). For the calculated part of the photoionization spectrum ($h\nu < 31E_d$) we have 0.60 (EMA), 0.65 (Sb), 0.76 (P), and 0.79 (As). With allowance for the transitions to highly excited levels with binding energies < 0.2 meV, the OS sum is very close to unity, just as in the case of donors in Si. The same regularity can be traced, viz, the fraction of the continuum increases with increase of E_i. Comparing the hydrogenlike atoms and donors in Si and Ge, it is easily noted that the fraction of the continuum also increases with decrease of γ. It must be borne in mind that in the limiting case of a two-dimensional hydrogenlike atoms its value is 0.721.

It is known[2] that if a multivalley semiconductor is uniaxially deformed along a direction corresponding in the Brillouin zone to a minimum of the conduction band, the ground state of the donor can be made to correspond to only one valley of the conduction band (in Ge) or to two valleys located on the same axis (in Si). To this end, the lowering δE_{def} of this valley by the deformation must be large compared with the valley-orbit interaction Δ. The cross section for optical absorption of the donors is then anisotropic, i.e., it depends on the polarization of the radiation relative to the valley axis, and the principal values of the cross-section tensor are equal to σ_t and σ_l. Figure 4 shows plots of the ratio σ_t/σ_l of different impurities in Ge and Si as functions of $h\nu/E_i$. It can be seen that the anisotropy of the photoeffect cross section is tremendous, especially for impurities with small Δ, for which it is easiest to meet the condition $|\delta E_{\text{def}}| \gg \Delta$. For example, the anisotropy of the Sb impurity in Ge exceeds 100, while that of Sb in Si should reach ~8. With increase of E_i the ratio σ_t/σ_l decreases at all $h\nu > E_i$, but it is large for all shallow donors, both in Ge and in Si. The fact that the cross section σ_t should be larger than σ_l follows from simple considerations: since $m_l > m_t$, the wave function of the donor is extended in the direction of the valley axis less than in transverse directions. According to the sum rule (10), the ratio of the total areas under the spectra σ_l and σ_t (including the line spectra) is equal to γ. The ratio σ_l/σ_t in the continuum, however, is even less than γ, for when γ decreases the fraction of that area under the σ_i spectrum that belongs to the continuous spectrum also decreases. It is equal to 0.11 in Ge (EMA), 0.17 in Sb, 0.32 in P, and 0.32 in As. The corresponding values in Si are 0.23 (EMA), 0.48 (Sb), 0.52 (P), and 0.62 (As), i.e., much lower than the fraction of the continuum in $\sigma_t(h\nu)$.

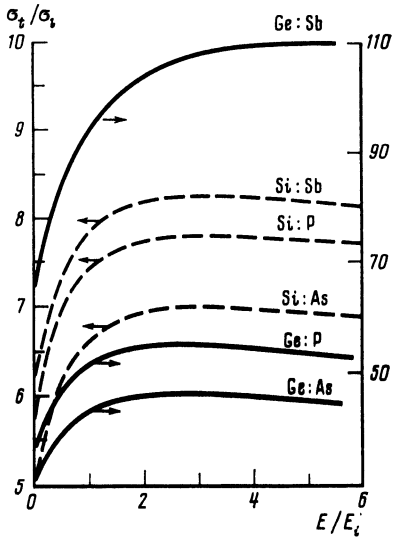

FIG. 4. Anisotropy of the cross section for donor photoionization in Ge (solid curves) and in Si (dashed) vs the photon energy.

5. POLARIZABILITY

The polarizability of an atomic system should equal, in order of magnitude, the cube of the effective radius of the wave function multiplied by the dielectric constant $\varkappa$. Since the radius of the wave function depends on the depth of the level, one should expect different chemical impurities to have different polarizabilities. Measurements made on donors in Si (see Table IV) confirm this (only the polarizability of Sb was measured for Ge, Ref. 30). Calculation of the polarizabilities of shallow donors in Si and Ge in the ZRCC approximation is of interest, since it makes it possible to assess, by comparing the results with the experimental data, the accuracy of this approximation. In addition, this is a convenient example that demonstrates the general effective method of calculating the polarizabilities (and, in general, quantities given by second-order perturbation theory) of non-hydrogenlike systems.

We consider the general equation for the polarizability tensor[31]:

$$\alpha_{ik}^{(n)} = 2 \sum_{n'(\neq n)} \frac{(d_i)_{nn'}(d_k)_{n'n}}{E_{n'} - E_n}. \tag{18}$$

Here ψ_n is the state of the system, and $(d_i)_{nn'}$ are the matrix elements of the dipole moment for a transition from ψ_n to other states $\psi_{n'}$ with energies $E_{n'}$. The task of calculating α_{ik} from (18) reduces to calculation of practically the entire optical spectrum. Since we calculated in the present paper the oscillator strengths of all the intense optical transitions in shallow donors and the photoionization spectrum, we might consider it possible to calculate the polarizabilities of the donors directly from (18). However, the contribution of the unaccounted-for excited states and the decrease of the accuracy of the OS calculation with increase of the number of levels make it more difficult to monitor the accuracy of α_{ik} as calculated from (18). More effective is a method that does not require calculation of the entire optical spectrum and is suitable also for calculation of other quantities given by second-order perturbation theory. We rewrite (18) in the form

$$\alpha_{ik}^{(n)} = 2\langle \psi^{(n)} | \hat{d}_i | \psi_k^{(n)} \rangle, \tag{19}$$

where $\psi_k^{(n)}$ is the solution of the inhomogeneous Schrödinger equation

$$(\hat{H}-E)\psi_k^{(n)}=\hat{d}_k\psi^{(n)}. \tag{20}$$

We proceed to dimensionless quantities and to the deformed coordinate frame in accordance with Eqs. (2). We confine ourselves for simplicity to calculation of the polarizability of the ground state (even, $M=0$). Let ψ_m ($m=0, \pm 1$) be the solution of the equation

$$(\hat{\tilde{H}}-\tilde{E})\psi_m=\tilde{x}_m\psi, \tag{20a}$$

in which $\tilde{x}_m$ is the component of an irreducible spherical tensor of first rank, ψ is the solution of (3), and $\tilde{\hat{H}}$ and $\tilde{E}$ are the dimensionless Hamiltonian (1) and the dimensionless energy. It follows from (2) and (19) that in a coordinate system connected with each individual valley the transverse and longitudinal polarizabilities are equal:

$$\alpha_t\equiv\alpha_{xx}=\alpha_{yy}=2\varkappa a^3\gamma^{-1/2}\langle\psi_1|\tilde{x}_1|\psi\rangle, \tag{21}$$
$$\alpha_l\equiv\alpha_{zz}=2\varkappa a^3\gamma^{1/2}\langle\psi_0|\tilde{x}_0|\psi\rangle.$$

In an underformed crystal, the polarizability of a donor that is in a ground singlet state is known to equal

$$\alpha=(2\alpha_t+\alpha_l)/3. \tag{22}$$

Since the function ψ in the right-hand side of (20a) is even and is characterized by an angular-momentum projection $M=0$, the expansion of ψ_m in spherical harmonics

$$\psi_m(\tilde{\mathbf{r}})=\sum_{L\geqslant 1} G_L^{(m)}(\tilde{r})\,Y_{Lm}(\theta,\varphi) \tag{23}$$

contains only functions with odd L and with $M=m=0, \pm 1$. From (20a) we get a system of equations for the radial functions:

$$-\frac{1}{2}\left[\frac{d^2}{d\tilde{r}^2}+\frac{2}{\tilde{r}}\frac{d}{d\tilde{r}}-\frac{L(L+1)}{\tilde{r}^2}+2\tilde{E}\right]G_L^{(m)} - \frac{1}{\tilde{r}}\sum_{L'} q_{LL'}^{(m)}\,G_{L'}^{(m)}-\tilde{r}\bar{R}_L^{(m)}(\tilde{r})=0. \tag{24}$$

Here $\bar{R}_L^{(m)}$ are given by Eqs. (14) and $q_{LL'}^{(m)}$ is a matrix element of $q(\theta)$ [Eq. (4)].

It is convenient to solve the set of equations (6) and (24) as a single system by the method of finite solutions at infinity. It follows from (5), (21), and (23) that

$$\alpha_t=2\varkappa a^3\gamma^{-1/2}\sum_{L\geqslant 1}\int_0^\infty d\tilde{r}\tilde{r}^3G_L^{(1)}(\tilde{r})\bar{R}_L^{(1)}(r),$$
$$\alpha_l=2\varkappa a^3\gamma^{1/2}\sum_{L\geqslant 1}\int_0^\infty d\tilde{r}\tilde{r}^3G_L^{(0)}(\tilde{r})\bar{R}_L^{(0)}(\tilde{r}). \tag{25}$$

The calculation results are listed in Table IV together with the experimental data (the values of α of the donors in Si have been refined many times; we list here the latest data). It can be seen that the polarizability of the donors depends very strongly on the depth of the ground level: if it is increased by approximately 70% compared with the EMA (As in Si) the value of α is decreased to one-sixth. The agreement with experiment is good: in almost all cases the deviation is less than the inaccuracy of the experiment itself, and only in the case of As in Si does the theoretical value go slightly beyond the limits of the experimental error.

A check on the sum rule in Sec. 4 has shown that the unaccounted-for highly excited states account for 1–3% of the total absorption. The values of α calculated directly from (18) with the aid of the OS obtained above and the photoeffect cross section should be expected to be lower by the same 1–3% than the values in Table IV. This was confirmed by the calculations.

We note only a few of the many calculations of α of donors in Si. A variational method was used in Ref. 32 to calculate α_t and α_l in the EMA. The results are close to those obtained by us for Si in the EMA. A variational method in the isotropic model yielded[33] the α of donors in Si by introducing in the Hamiltonian a model short-range (center-cell) potential whose parameter was chosen for each donor in such a way that the ground-state energy was equal to the known E_i. A similar calculation of α of the isotropic model, but by the quantum-defect method, was carried out in Ref. 29. It is interesting that the values of α obtained in Refs. 33 and 29 for the isotropic model of the donor are very close to those obtained by us with allowance for the mass anisotropy. This agreement may be accidental, since other properties of the donors, calculated in the isotropic model, differ substantially from the exact ones (see Sec. 4). In addition, it is impossible to calculate α_t and α_l separately in the isotropic model.

6. EFFECT OF MAGNETIC FIELD ON THE VALLEY-ORBIT LEVEL SPLITTING

We know that, in a semiconductor whose conduction band has n_v valleys, the ground state of a shallow donor is n_v-fold degenerate in the EMA, and that this degeneracy is partially lifted by center-cell correction (by valley-orbit interaction). The fourfold degenerate level in Ge is split into a singlet A_1 and a triplet T_2, and the sixfold degenerate level in Si is split into a singlet A_1, doublet E, and triplet T_2 (Refs. 34 and 2). Let us see how a magnetic field **B** influences the distances between these levels.

There are no orbital-motion level-shifts that are linear in B, since in all the foregoing states the projection of the angular momentum on the valley axis is $M=0$. On the other hand, the diamagnetic level shifts ($\sim B^2$) are not alike: they are larger the higher the level and hence the larger the extent of its wave function. Therefore the valley-orbit level splitting in a magnetic field increases, and furthermore the degenerate levels are split if B is not symmetrically oriented relative to all the valleys of the conduction band. The effect of the valley-orbit splitting dependence $4\Delta(B)$ was measured for **P** and **As** donors in Ge.[35,36] This dependence is used to interpret experiments on the phonon thermal conductivity of Ge with shallow donors in a magnetic field.[37,38] Since the quantity $4\Delta(B)-4\Delta(0)$ depends directly at small B on the behavior of the wave functions of the ground levels, we can, by comparing the effect calculated in the ZRCC approximation with experiment, check quantitatively the accuracy of this approximation.

In the presence of a magnetic field, it is necessary to add to the Hamiltonian (1) of an electron in each valley the following energy operators:

$$\hat{H}_{B1}=\frac{e\hbar}{2ic}\left\{\frac{1}{m_t}z[\mathbf{B}\nabla]_z+\frac{1}{m_t}B_z\frac{\partial}{\partial\varphi}+\frac{1}{m_l}[\mathbf{Br}]_z\frac{\partial}{\partial z}\right\}, \tag{26}$$

TABLE IV. Shallow-donor polarizability in Si and Ge (in units of 10^5 Å^3).

Impuurity	Si				Ge			
	α_t	α_l	α	α_{exp}	α_t	α_l	α	α_{exp}
EMA	5.35	2.26	4.32	–	108	21.0	79.2	–
Sb	1.96	0.70	1.54	1.9±0.6 [27]	88.0	15.7	63.9	68±15 [30]
P	1.61	0.56	1.26	1.1±0.1 [28] 1.2±0.2 [27]	45.7	6.50	32.6	–
As	0.96	0.31	0.74	0.52±0.09 [29]	34.6	4.55	24.6	–

$$\hat{H}_{B2}=\frac{e^2}{8m_tc^2}\{B^2r^2-(\mathbf{Br})^2-(1-\gamma)\times[B_\perp^2(x^2+y^2)-(B_xx+B_yy)^2]\}. \quad (27)$$

Contributions to the level shifts are made by perturbation theory of first order in H_{B2} and of second order in H_{B1}.

We denote by angle brackets the averaging of the effective mass with a given level energy at $B=0$ over the solution ψ of Eq. (3). It follows from (27) and (2) that

$$\langle\hat{H}_{B2}\rangle_v=\left(\frac{\hbar eB}{m_tc}\right)^2\frac{1}{E_d}\left[h_2^{(0)}+h_2^{(2)}\left(b_{zv}^2-\frac{1}{3}\right)\right]. \quad (28)$$

Here b_{zv} is the component of the vector $\mathbf{b}=\mathbf{B}/B$ on the Z axis of valley v,

$$h_2^{(0)}=\frac{1}{36}\left[(1+2\gamma)\langle\tilde{r}^2\rangle-(1-\gamma)\left\langle\tilde{r}^2\left(\frac{3}{2}\cos^2\theta-\frac{1}{2}\right)\right\rangle\right],$$
$$h_2^{(2)}=\frac{1}{12}\left[(1-\gamma)\langle\tilde{r}^2\rangle-\left(1+\frac{\gamma}{2}\right)\left\langle\tilde{r}^2\left(\frac{3}{2}\cos^2\theta-\frac{1}{2}\right)\right\rangle\right]. \quad (29)$$

We represent the energy correction of second order in H_{B1} in the form

$$2\langle\hat{H}_{B1}(E-\hat{H})^{-1}\hat{H}_{B1}\rangle_v=\left(\frac{\hbar eB}{m_tc}\right)^2\frac{1}{E_d}h_1(1-b_{zv}^2), \quad (30)$$

where

$$h_1=\frac{\gamma}{2}\langle\psi|\hat{H}_1|\chi\rangle, \quad (\hat{H}-E)\chi=-\hat{H}_1\psi, \quad (31)$$

H_1 is the dimensionless Hamiltonian H_{B1}. The procedure of calculating h_1 with the aid of (3) and (31) is similar to the procedure of calculating the polarizability (see Sec. 5).

If the field **B** is symmetrically oriented relative to all the valleys, it only shifts the levels but does not split the nondegenerate levels T_2 and E. The shift of each level is equal to βB^2, where

$$\beta=\left(\frac{\hbar e}{m_tc}\right)^2\frac{1}{E_d}\left(h_2^{(0)}+\frac{2}{3}h_1\right). \quad (32)$$

The calculated values of this quantity for the donor levels in Ge and Si are listed in Table V, which gives also (for Ge) the measured value of

$$\Delta\beta=\beta(1sT_2)-\beta(1sA_1)=[4\Delta B-4\Delta(0)]/B^2. \quad (33)$$

It is seen from the data of Table V that the values of $\Delta\beta$ calculated in the ZRCC approximation differ from the experimental value by approximately the error of the experiment itself ($\sim 10\%$). At the same time the value of $\Delta\beta$ obtained in those of the known calculations[37,39] of the effect, in which no special assumptions were made to obtain agreement with experiment, is approximately three times larger than the experimental one. (The reason is that the valley-orbit interaction was treated in these calculations as a perturbation.)

7. ESTIMATED ACCURACY OF THE ZRCC APPROXIMATION FOR SHALLOW DONORS IN GERMANIUM AND SILICON

We have found in Sec. 5 that the shallow-donor polarizabilities calculated in the ZRCC approximation differ from the experimental values by amounts of the order of the error of the experiment itself, i.e., by 10–30%. This means that the accuracy of the ZRCC approximation is quite high in this case—not worse than $\sim 10\%$ (the accuracy of the numerical calculation is even higher, on the order of 1%). Since the polarizability of the impurity atom is expressed in terms of the same dipole-moment matrix elements that determine the spectral-line intensities and the photoionization cross section, one should expect the accuracy of the ZRCC-approximation calculation of these values for shallow donors in silicon to be likewise not worse than $\sim 10\%$.

From among the quantities that depend on the form of the wave function of the ground state of shallow donors in germanium, the most accurately ($\sim 10\%$) measured is the quadratic change $\Delta\beta$ of the valley-orbit splitting in a magnetic field (see Sec. 6). The errors in the calculated values of $\Delta\beta$ of P and As impurities in Ge exceed, albeit little, the $\sim 10\%$ experimental error. At the same time, the ratio a_0/a of the dimension of the center cell to the effective Bohr radius is smaller in Ge than in Si, and one might expect the ZRCC approximation to be more accurate for Ge. It is possible that the measured $\Delta\beta$ receives also a contribution from some effect not accounted for by us. A more accurate estimate of the ZRCC approximation for donors in germanium will be possible after the oscillator strengths of the lines in the absorption spectrum and the cross sections for photoionization of shallow donors are measured with higher accuracy.

The authors are grateful to A. F. Polupanov for valuable advice and numerous discussions of the work. The authors are also grateful to B. L. Gel'mont, M. I. D'yakonov, E. L. Ivchenko, L. V. Keldysh, V. I. Perel', and G. E. Pikus for a discussion of individual results of the work.

APPENDIX

By making the substitutions $R_i=y_i$ and $rR_i'=y_{i+N}$ one can represent the system (6) in the form of a system of $2N$ first-order ordinary differential equations:

TABLE V. Values of β, which determine the quadratic shifts of the donor levels in a magnetic field (in μ eV/T^2).

Impurity	Ge				Si		
	$\beta(A_1)$	$\beta(T_2)$	$\Delta\beta$	$\Delta\beta_{exp}$ [35,36]	$\beta(A_1)$	$\beta(E)$	$\beta(T_2)$
P	5,10	7,93	2,83	2,32±0,25	0,339	0,614	0,572
As	4,33	8,11	3,78	3,35±0,25	0,256	0,663	0,612
Sb	7,38	7,81	0,43	–	0,378	0,694	0,604

$$y_i' = \left(\frac{1}{r}A_{ik}^{(0)} + A_{ik}^{(1)} + rA_{ik}^{(2)}\right)y_k, \qquad (A.1)$$

in which the matrices $A^{(0)}$, $A^{(1)}$, and $A^{(2)}$ are independent of the radial variable r.

We solve the eigenvalue problem:

$$U_{mj}A_{ji}^{(0)} = \lambda_m U_{mi}. \qquad (A.2)$$

If the system (6) pertains to the ground state ($L = 0, 2, 4, \ldots L_{max}$) the numbers λ_m take on N positive (0,2, ... L_{max}) values and N negative ones ($-1, -3, \ldots, -L_{max}-1$). The condition that the solution be bounded at $r = 0$ takes the form of N equations ($\lambda_m < 0$):

$$U_{mi}y_i(0) = 0. \qquad (A.3)$$

If, however, the solution must diverge not faster than r^{-1}, it is necessary to discard from (A.3) the condition that corresponds to $\lambda_m = -1$ (Ref. 10). The remaining $N-1$ conditions together with the N conditions that the solutions be finite at infinity determine uniquely the solution if the energy E is known (from experiment). The functions $y_i(r)$ are calculated by the method of finite-solutions conditions at the point $r = 0$ and the requirement that the solution tend at $r \to \infty$ to a finite point (Refs. 8–10). If the energy E does not coincide with an eigenvalue of the system (6) or with (A.1), the solution obtained by this method diverges as $r \to 0$ like r^{-1} and is therefore normalizable.

[1)]After submitting this article, the authors beame acquainted with Ref. 13, in which a variational calculation much more accurate than in Ref. 12 was made, and the existence of the experimentally unobserved levels $6P_{\pm}$ and $9P_{\pm}$ was concluded. No oscillator strengths were found in Ref. 13, however.

[1]J. M. Luttinger and W. Kohn, Phys. Rev. **97**, 869 (1955).
[2]G. L. Bir and G. E. Pikus, *Symmetry and Strain-Induced Effects in Semiconductors*, Wiley, 1975.
[3]S. T. Pantelides, Rev. Mod. Phys. **50**, 797 (1978).
[4]W. Kohn and J. M. Luttinger, Phys. Rev. **97**, 883 (1966).
[5]Sh. M. Kogan and A. F. Polupanov, Zh. Eksp. Teor. Fiz. **80**, 394 (1981) [Sov. Phys. JETP **53**, 201 (1981).
[6]Sh. M. Kogan and R. Taskinboev, Fiz. Tekh. Poluprovod. **17**, 1583 (1983) [Sov. Phys. Semicond. **17**, 1007 (1983)].
[7]A. R. Edmonds, *Angular Momentum in Quantum Mechanics*, Princeton, 1957.
[8]A. A. Abramov, B. B. Ditkin, N. B. Konyukhov, B. S. Pariiskiĭ, and V. I. Ul'yanova, Zh. vych. Mat.i mat. fiz. **20**, 1155 (1980).
[9]Yu. A. Kurskiĭ, B. S. Pariiskiĭ, and R. Taskinboev, Applied Mathematics Communications [in Russian], Comp. Center, USSR Acad. Sci. 1980.
[10]I. L. Beinikhes, Sh. M. Kogan, A. F. Polupanov, and R. Taskinboev, Sol. St. Comm. **53**, 1083 (1985).
[11]Sh. M. Kogan and A. F. Polupanov, *ibid.* **27**, 1281 (1978).
[12]R. A. Faulkner, Phys. Rev. **184**, 713 (1969).
[13]J. Broeckz, P. Clauws, and J. Vennik, J. Phys. **C19**, 511 (1986).
[14]M. S. Seecombe and D. M. Korn, Sol. St. Comm. **11**, 1539 (1972).
[15]M. S. Skolnik, L. Eavens, R. A. Stradling, *et al.*, *ibid.* **15**, 1403 (1974).
[16]I. L. Beĭnikhes and Sh. M. Kogan, Pis'ma Zh. Eksp. Teor. Fiz. **44**, 39 (1986) [JETP Lett. **44**, 48 (1986)].
[17]B. Pajot, J. Kauppinen, and R. Anttila, Sol. St. Comm. **31**, 759 (1979).
[18]C. Jagannath, Z. W. Grabowski, and A. K. Ramdas, Phys. Rev. **B23**, 2082 (1981).
[19]W. H. Kleiner and W. E. Krag, Phys. Rev. Lett. **23**, 2082 (1970).
[20]I. L. Beĭnikhes and Sh. M. Kogan, Zh. Eksp. Teor. Fiz. **89**, 722 (1985) [Sov. Phys. JETP **62**, 415 (1985).
[21]H. B. Bebb, Phys. Rev. **185**, 1116 (1969).
[22]D. D. Coon and R. P. G. Karunasiry, Phys. Rev. **B33**, 8228 (1986).
[23]G. Picus, E. Burstein, and B. Henvis, J. Phys. Chem. Sol. **1**, 75 (1956).
[24]R. Baron, M. H. Young, J. K. Neeland *et al.*, Appl. Phys. Lett. **30**, 594 (1977).
[25]J. H. Reuszer and P. Fischer, Phys. Rev. **140**, A245 (1965).
[26]P. A. Bratt, Infrared Detectors, Part II. Semiconductors and Semimetals, Vol. 12 (R. K. Willardson and A. C. Beer, eds.), Academic, 1977, p. 39.
[27]H. S. Tan and G. Kasiner, Phys. Rev. **B23**, 3983 (1981).
[28]M. Capizzi, G. A. Thomas, F. DeRose *et al.*, Phys. Rev. Lett. **44**, 1019 (1980).
[29]R. J. Deri and T. G. Castner, Phys. Rev. **B33**, 2796 (1986).
[30]F. A. D'Altroy and Y. Y. Fan, Phys. Rev. **103**, 1671 (1956).
[31]L. D. Landau and E. M. Lifshitz, Quantum Mechanics, Nonrelativistic Theory, Pergamon, 1978, p. 265.
[32]D. L. Dexter. Proc. 13th Internat. Semicond. Conf. (F. G. Fumi, ed.), Rome, 1976, p. 1137.
[33]N. O. Lipari and D. L. Dexter, Phys. Rev. **B18**, 1346 (1978).
[34]W. Kohn and J. M. Luttinger, Phys. Rev. **98**, 915 (1955).
[35]R. L. Aggarwal, Physics of High Magnetic Fields, Proc. Oji Int. Seminar, Hakone, Sept. 10–13 (1980). Springer, 1081, p. 105.
[36]C. Jagganath, R. L. Aggarwal, and D. M. Larsen, Sol. St. Comm. **53**, 1089 (1985).
[37]L. Halbo, *Phonon Scattering in Solids*, L. J. Challis *et al.*, eds. Plenum, 1976, p. 346.
[38]S. Singh and G. S. Verma, Phys. Rev. **B19**, 5433 (1979).
[39]N. Lee, D. M. Larsen, and B. Lax, J. Phys. Chem. Sol. **34**, 1817 (1973).

Translated by J. G. Adashko